Mongolian Geoscientist

Original Article

Impact of faulting on the depression morphology of Ulaagchinii Khar Lake in Mongolia

Altanbold Enkhbold[1], Ulambadrakh Khukhuudei[2]*, Yeong Bae Seong[3], Daariimaa Badarch[2], Ser-Od Tsedevdorj[4], Batzorig Batbold[1], Byambabayar Ganbold[1]

[1]Laboratory of Geopedology, Department of Geography, School of Art and Sciences, National University of Mongolia, Ulaanbaatar 210646, Mongolia
[2]Research Center of Geology and Mineral Resources, and Department of Geology and Geophysics, School of Arts and Sciences, National University of Mongolia, Ulaanbaatar 210646, Mongolia
[3] Department of Geography Education, Korea University, Seoul 02841, Korea
[4] Department of Geography, School of Mathematics and Natural Sciences, Mongolian National University of Education, Ulaanbaatar, 14191, Mongolia

*Corresponding author: ulambadrakh@num.edu.mn, ORCID: 0000-0003-4570-7053

ARTICLE INFO

Article history:

Received: 30 December, 2024
Revised: 09 April, 2025
Accepted: 18 May, 2025

ABSTRACT

The geomorphology of the Ulaagchinii Khar Lake depression is predominantly governed by tectonic faulting. Morphometric analysis identifies a distinct network of orthogonal faults that are prominently manifested in both topographic and bathymetric patterns. These fault systems primarily trend northwest-southeast and north-south, intersecting near the lake's central region. This central zone is characterized by pronounced linear formations and abrupt shifts in elevation, as depicted in isobath profiles, indicative of tectonic subsidence along fault zones. The lake depression exhibits strong tectonic control, supported by a high hypsometric integral (*HI*=0.91) and a notably elongated basin shape index (*Bs*=2.81). Further evidence for a tectonic origin includes a major east-west oriented fault extending 40.8 km with a steep inclination of 35°, and a vertical relief energy of 274 m. Significant depth variations, reaching up to 47 m in the lake's western sector, further reinforce the influence of faulting on its morphological configuration. Complementary geomagnetic anomaly data also correspond with these structural features, affirming the presence of active tectonic processes within the depression. The orthogonal fault systems have not only shaped the physical structure of the depression but have also influenced its hydrological regime by enhancing groundwater infiltration, thereby contributing to the lake's freshwater characteristics. This research underscores that the current morphology and hydrological compartmentalization of Ulaagchinii Khar Lake are the result of an interplay between tectonically controlled fault activity and Late Quaternary dune deposition

Keywords: Khangai Mountain, Morphometric analysis, Sobel filter, Lake depression, Magnetic anomaly, Bor Khyar dune

INTRODUCTION

The investigation into the origins of lake depressions holds both scientific relevance and practical implications (Cohen, 2003), as the natural conditions and resource potential of a lake are inherently connected to the genesis and fundamental attributes of its depression. The development of lake basins reflects the combined impact of endogenic and exogenic geological processes, which collectively shape their contemporary morphology (Mats, 1993; Shamir, 2006).

Globally, research into the genesis of lake depressions began approximately 130 years ago (Cohen, 2003). In contrast, the study of Mongolian lake depressions has a comparatively shorter history, spanning around five decades (Tserensodnom, 1971, 2000; Enkhbold et

al., 2021a). The majority of Mongolia's significant lake systems are situated in the western region, predominantly aligned with extensive intermontane basins (Tsegmid, 1969; Tserensodnom, 1971; Grunert et al., 2000; Shinneman et al., 2009; Enkhbold et al., 2021a; Enkhbold et al., 2024a). Traditionally, the origins of these depressions have been classified into tectonic, volcanic, glacial, landslide-dammed, aeolian, and fluvial types (Tserensodnom, 1971, 2000). More recently, Enkhbold et al. (2021a) proposed a refined classification system encompassing eight distinct primary types, offering a more nuanced perspective than earlier frameworks. Comparative analyses of these classification systems reveal that tectonic processes are the dominant contributors to the formation of Mongolian lake depressions (Enkhbold et al., 2021a).

While numerous studies have investigated fault-related structures across Mongolia (e.g., Bayasgalan et al., 1999; Lamb et al., 1999; Carretier et al., 2002; Cunningham et al., 2003; Bayasgalan et al., 2005; Cunningham, 2005; Walker et al., 2007; Nissen et al., 2007; Walker et al., 2008; Byamba, 2009; Cunningham, 2013), their specific influence on the morphological development of lake depressions remains largely unexplored. At the current stage of research, the classification of the Ulaagchinii Khar Lake (UKL) depression remains tentative and insufficiently substantiated, as evidenced by our findings. Given the lake's significance as a major site for tourism and recreation in Mongolia, a precise and comprehensive understanding of its origin is essential for both scientific advancement and practical applications.

Previous interpretations attributed the formation of the UKL depression to aeolian processes (Tserensodnom, 1971, 2000). However, our study presents a divergent perspective, emphasizing the need for in-depth investigations to elucidate the origins and morphological characteristics of over 3,000 lake depressions throughout Mongolia.

The aim of this study is to comprehensively determine the origin and morphological characteristics of the UKL depression by integrating morphometric analysis, satellite, geophysical map interpretation, and field measurement results, with a particular focus on assessing the influence of faulting on its formation and morphology.

Study Area

The UKL depression is located in central-western Mongolia, at the transitional boundary between arid steppe and semi-arid mountainous zones (Tsegmid, 1969; Enkhbold et al., 2024b). Positioned at the terminal point of the Bor Khyar dunefiled, the lake lies approximately 80 km north of Erdenekhairkhan soum in Zavkhan Province. Geographically, it is situated at 48°20′34″N latitude and 96°06′46″E longitude, with an elevation of roughly 1,980 m above sea level (m a.s.l.). UKL spans a surface area of 84.5 km² and contains freshwater. The lake extends 23.9 km along a west-east axis and has an average width of 3.5 km. Its shoreline measures 64.7 km in length. The lake reaches a maximum depth of 47 m in its western section and about 30 m in the eastern part, with a total estimated water volume of 1.65 km³ (Tserensodnom, 2000). It receives inflow from the Ulaagchinii River entering from the east, while no external outlet is present (Fig. 1).

From a geological perspective, the southern section of the UKL is underlain by Neoproterozoic gabbroid complexes, whereas the northern part is primarily composed of Devonian granitoids (Samozavntsev et al., 1981). These bedrock units are encircled by Late Quaternary unefield (Tserensodnom, 1971). Geomorphologically, the region is characterized by lacustrine plains in the immediate vicinity of the lake, transitioning into low to mid-altitude mountains, which exhibit significant dissection in the southern sector (Tsegmid, 1969; Doljin and Yembuu, 2021). Extensive aeolian sand deposits dominate the landscape surrounding the lake (Tserensodnom, 2000). The inflow of the Ulaagchinii River is partially impeded by these sand accumulations, contributing to distinct morphological features on the lake's surface. Nevertheless, findings from this study indicate that tectonic processes exert a more pronounced influence on the formation of the lake depression than aeolian dynamics.

The UKL depression spans approximately 39.7

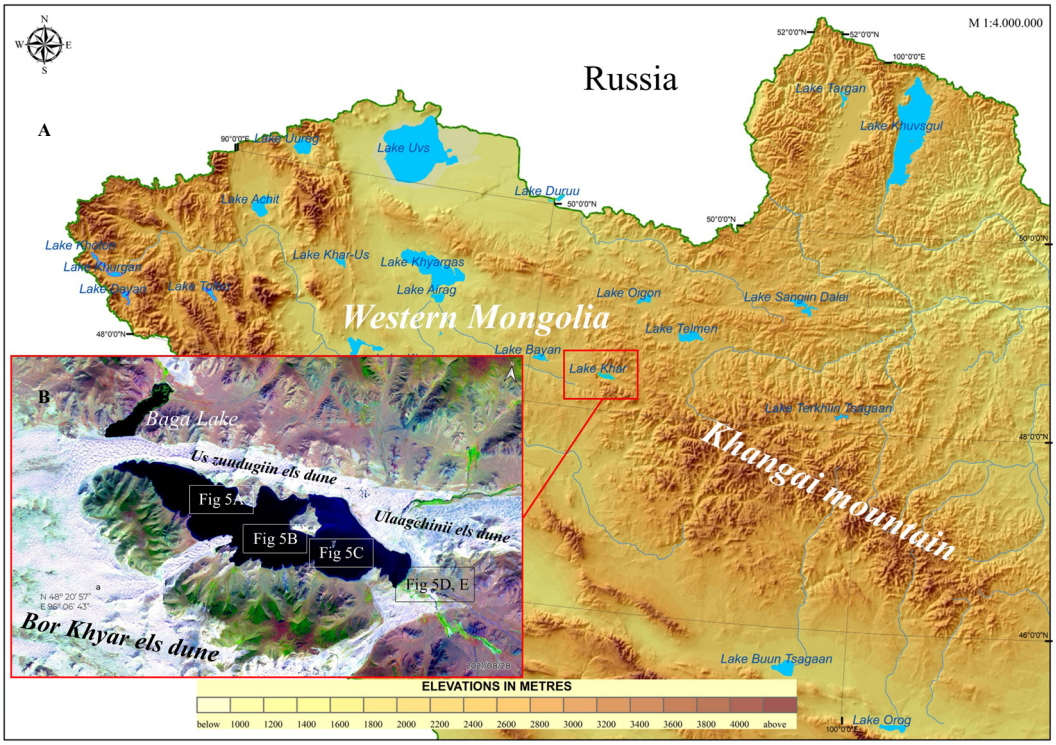

Fig. 1. Location of the Study Area. A -Distribution of lakes in Western Mongolia, B -Satellite image of UKL and Bor Khyar dune (modifeid after Enkhbold et al., 2022b), (Field measurement images are presented in Fig. 5)

km in length and 14.1 km in width, encompassing a total area of 378.4 km². The lowest point within the depression lies at 1,934 m above sea level (m a.s.l.), while the surrounding highlands reach elevations of up to 2,208 m. This significant variation in elevation is attributed to both tectonic activity and erosional forces that have shaped the depression's geomorphological development. According to geomorphological classification, the lake is situated within the Khangai zone of the Khangai Mountainous Region (Enkhbold et al., 2024b).

MATERIALS AND METHODS

This study integrated multiple datasets, including 1:100,000 scale topographic maps, lake bathymetric maps (Sevastyanov et al., 1994; Tserensodnom, 2000), Landsat OLI satellite imagery (30 m resolution), 1:250,000 scale vertical geomagnetic anomaly gradient maps, and 1:200,000 scale geological maps of lake depressions. Field investigations comprised morphometric measurements and water sampling, with chemical analyses of the water samples conducted at the "Green Lab" LLC laboratory.

A cross-sectional profile of the lake depression was developed along its most prominent fault line, spanning 10 km. This profile enabled the identification of geological structures and fault boundaries intersecting the depression, supporting the morphological interpretation through modeled reconstruction.

Morphometric Analysis: The identification of faults within lake depressions via morphometric analysis presents considerable complexity, yet remains essential (Karatas and Boulton, 2019). Topographic analysis (TA) of morphometric indicators such as anomalous relief patterns, spatial distribution of anomalies, and deviations from typical surface features can enhance the likelihood of fault detection (Florinsky, 1996; Enkhbold et al., 2024a). Relief discontinuities, horizontal and vertical displacements, degrees of fault activity, and deformation features indicative of slicing are all key morphometric markers of neotectonic activity.

Among the various morphometric approaches, this study employed the method developed by Filosofov (1967), which is particularly effective in detecting neotectonic movements by analyzing topographic maps and interpreting landform genesis. Variations in contour elevations indicative of vertical displacements or the presence of linear relief structures

suggest faulting associated with endogenous processes (Yang et al., 2015; Enkhbold et al., 2022b, 2022c). On topographic maps, tightly spaced contours and the presence of linear alignments are typically associated with fault zones (Enkhbold et al., 2021b). Accordingly, morphometric analysis of the UKL depression's relief was conducted using precise measurements and interpretations based on topographic maps (Filosofov, 1967; Jacques et al., 2014), with topographic analysis serving as a central component of the methodological framework.

The hypsometric integral (*HI*) is a dimensionless metric used to assess the relative distribution of elevation within a given depression. It is calculated using the formula:

$$HI\,(\%) = \frac{E_{mean} - E_{min}}{E_{max} - E_{min}} \quad (1)$$

where E_{mean} is the mean elevation, E_{min} is the minimum elevation, and E_{max} is the maximum elevation of the depression (Strahler, 1964; Farhan et al., 2016; Maliqi et al., 2023). A high *HI* value (>0.5) generally indicates a tectonically active landscape dominated by uplift, whereas a low *HI* value (<0.4) is typically associated with geomorphologically mature or stable terrains, shaped predominantly by long-term erosional processes (Hassen et al., 2014; Jacques et al., 2014; Enkhbold et al., 2021b).

The basin shape index (*Bs*) is another morphometric parameter often utilized to evaluate tectonic influence on landscape evolution, particularly in mountainous regions. In tectonically active areas, basins tend to exhibit elongated shapes, which gradually transition toward more circular forms over time due to erosional processes (El Hamdouni et al., 2008; Anand and Pradhan, 2019). The basin shape index is defined as:

$$Bs = \frac{Bl}{Bw} \quad (2)$$

where *Bl* represents the total basin length from the headwater to the outlet, and *Bw* denotes the basin width at its widest point (El Hamdouni et al., 2008; Anand and Pradhan, 2019; Das et al., 2022).

Table 1. Basin shape (*Bs*) index values used to classify tectonic activity levels (El Hamdouni et al., 2008; Anand and Pradhan, 2019; Das et al., 2022)

Tectonic activity	*Bs* index	Basin shape
Highly	≥ 2.3	Elongated
Moderately	1.2 to 2.3	Less elongated or oval
Less or inactive	≤ 1.2	Circular

The relief slope (*RSl*) analysis can be recognized by distinct discontinuities in relative height and steep side slopes, as indicated by the hypsometric curve (Ganas et al., 2005; Onorato et al., 2017). The hypsometric curve, which can be derived from satellite-based Google earth pro, quantifies *RSl* values. The likelihood of fault presence can be assessed based on surface slope characteristics within the lake depression. Specifically, *RSl* values indicate different probabilities of faulting: *RSl*<5° is low probability of faulting, 5°<*RSl*<10° is possible fault presence, and *RSl* >10° is the high probability of a fault (Hooper et al., 2003; Ganas et al., 2005; Onorato et al., 2017; Enkhbold et al., 2021b).

The relief energy (*RE*) indicators provides another method for fault identification on lake depression. *RE* represents the difference in relative height across the surface (Di Crescenzo and Santo, 2005). The *RE* value is calculated using the following equation:

$$RE = H_{max} - H_{min} \quad (3)$$

where *RE* is the Relief Energy (m), H_{max} is the maximum surface height (m), and H_{min} is them inimum surface height (m). A sharp increase in *RE* values suggests a higher likelihood of fault association with the lake depression surface (Di Crescenzo and Santo, 2005; Enkhbold et al., 2021b; Enkhbold et al., 2022b).

Spatial improvement method (Sobel filter): Geological interpretation using numerical data of specific surface areas, including satellite imagery, relies on the interpretation of geomorphological features depicted on the surface. This method is based on clarifying the features through all possible criteria that

can be interpreted, integrating the results for a comprehensive conclusion (Launay and Guerif, 2005; Theilen-Willige et al., 2016; Nixon and Aguado, 2019). In this study, we identified and interpreted faults visible on the surface. The equation for spatial improvement is defined as follows:

$$G_{j,k}=/G_X/+/G_Y/ \quad (4)$$

$$G_X=F_{j+1,\,k+1}+2F_{j+1,\,k}+F_{j+1,\,k-1}-(F_{j-1,\,k+1}+2F_{j-1,\,k}+F_{j-1,\,k-1}) \quad (5)$$

$$G_Y=F_{j-1,\,k-1}+2F_{j,\,k-1}+F_{j+1,\,k-1}-(F_{j-1,\,k+1}+2F_{j,\,k+1}+F_{j+1,\,k+1}) \quad (6)$$

Here, $(j,\ k)$ refers to the precise values of each pixel F_{jk} on the satellite image. These are determined by mapping them onto the image using the following matrix masks.

$$Y\ mask = \begin{matrix} 1 & 2 & 1 \\ 0 & 0 & 0 \\ -1 & -2 & -1 \end{matrix} \qquad X\ mask = \begin{matrix} -1 & 0 & 1 \\ -2 & 0 & 2 \\ -1 & 0 & 1 \end{matrix} \quad (7)$$

In spatial improvement, the value of each pixel is adjusted based on the surrounding pixels. To do this, windows of various sizes, referred to as kernels, are selected. The window moves along the rows and columns of the image, and whenever it reaches a specific pixel, the value of the kernel's center is redefined using the values of the other pixels within the window. In this way, the radiometric values of each pixel in the image are modified, enhancing the spatial representation of natural and anthropogenic features depicted on the image (Jensen 1996, Canty, 2014; Gilvear and Bryant, 2016). Using this method, two types of directional filters can be applied to compute the results of the study.

Directional Filter 1: This function enhances the original boundaries and clarifies specific features of the image along a certain direction. The sum of the kernel elements of the directional filter equals zero. As a result, pixels with uniform values in the newly generated image will have a value of zero, while features appearing in a specific direction will be represented as sharp and distinct values.

Directional Filter 2: The directional filter enhances edge features and is used by calculating the original features of the image. The original features generate significant differences between adjacent pixels, which are clearly visible on processed satellite images.

These directional filters were applied to satellite imagery of varying spatial resolutions using the *Directional Filter* tool available under the *Convolution and Morphology* module in ENVI 5.3 remote sensing software. The method facilitated the enhancement and mapping of fault lines within the lake depression.

Geophysical Magnetic Field Mapping: Magnetic anomaly mapping of the Earth's magnetic field is a widely utilized method in geological studies, particularly for identifying faults and tectonic boundaries (Boyce et al., 2002; Salem et al., 2008). Magnetic field surveys are instrumental in delineating tectonic fractures, as well as determining their orientation, extent, and depth (Tsagaan et al., 2024). The numerical values derived from magnetic field measurements offer critical insights into subsurface geological features, including variations in lithology and the presence of fault zones.

Geophysical magnetic field data represent a composite signal produced by all subsurface magnetic sources. In this context, a magnetic anomaly can be understood as a superposition of multiple harmonic components of differing frequencies and spatial extents, each corresponding to sources at varying crustal depths (Studinger et al., 2003). Consequently, parameters such as the depth and dip direction of fault-related anomalies can be estimated using spectral analysis techniques (Salem et al., 2008).

In other words, fault parameters can be identified using mathematical techniques based on data coming from different depths of the geophysical magnetic anomaly.

The horizontal and vertical components of the geophysical magnetic anomaly, as well as the total horizontal component, are used to detect faults through the analytical signal values (Phillips, 2000). If $f(r)$ represents a potential field depending on space and time, its Fourier transform to a frequency function can be represented as $F(k)$, as follows:

$$F_{(k)} = \frac{1}{\sqrt{2\pi}} \int_{-\infty}^{\infty} f_{(r)} e^{ik \cdot r} \, d^3\mathrm{r} \quad (8)$$

Here, r is the coordinate vector, and k is the wave number vector.

$$\frac{\partial f_{(r)}}{\partial x} = \int_{-\infty}^{\infty} ikF(k)\, e^{-ik \cdot r} d^3k \quad (9)$$

The analytic signal of the potential field *f(r)* is defined as follows:

$$AS = \sqrt{\left(\frac{\partial f_{(r)}}{\partial x}\right)^2 + \left(\frac{\partial f_{(r)}}{\partial y}\right)^2 + \left(\frac{\partial f_{(r)}}{\partial z}\right)^2} \quad (10)$$

RESULT AND DISCUSSION

Morphometric and Satellite Map Interpretation: To assess the extent to which faults influence the morphology of the UKL depression, geomorphological interpretation through topographic analysis was conducted. This method employs key topographic parameters such as elevation, slope, and contour configuration to detect geomorphic anomalies and structural lineaments indicative of tectonic activity.

Analysis of the topographic map revealed several noteworthy features. In the central sector of the lake, closely spaced contour lines delineate a prominent linear structure, suggesting abrupt relief changes. A distinct anomaly was observed along the mid-contour elevations, forming a clear linear displacement pattern. This feature aligns spatially with a linear formation present in both the relief and bathymetric contours near Ikh Abgash Island and Elst Shanaa Mountain (2,179.2 m). The presence of steeply descending isobaths in this area strongly implies fault-controlled subsidence. Moreover, the bathymetric contours exhibit a stepped, linear structure, with several parallel alignments corresponding to the main topographic contours, reinforcing the interpretation of faulting.

In the western portion of the lake, similar patterns were identified. Specifically, the contour spacing near the eastern flank of Deed Nam Mountain (2,273 m) and Elst Shanaa Mountain indicated abrupt elevation changes. Bathymetric profiles in this region also revealed a sharp descent, accompanied by a pronounced elevation anomaly within the contour spacing near the Avdrant ravine, suggesting an underlying fault structure. At the convergence of multiple fault lines on the lake's western side, a rapid increase in depth (up to 47 m) was observed further supporting the hypothesis of tectonic subsidence in this zone (Fig. 2A).

The hypsometric integral (HI) for the UKL depression was calculated at 0.91, indicating a relatively youthful geomorphic surface and supporting the interpretation of active tectonic processes (Fig. 2B). Additionally, the basin shape index (Bs) was determined to be 2.81, indicative of an elongated oval basin, commonly associated with tectonically influenced depressions. A major latitudinal fault, extending approximately 40.8 km, exhibits a steep slope gradient (RSL) of 35°, as measured along the A-A' cross-sectional transect from 2,050 m to the lake's deepest bathymetric point. Relative elevation (Re) analysis further revealed a vertical relief of 274 m within the depression. Collectively, these morphometric indicators confirm a significant tectonic influence on the formation and ongoing evolution of the UKL depression.

Satellite imagery was also utilized to enhance the detection of structural features. High-resolution spatial enhancement techniques were applied to highlight linear spectral anomalies that correspond to tectonic faults (Theilen-Willige et al., 2016). These techniques enhance contrast by emphasizing abrupt pixel intensity transitions, often associated with faulting. Directional filters aligned with the expected orientations of regional faults (e.g., the Kharnuur fault trending NW-SE, and an orthogonal N-S fault) were applied to the satellite data. These high-frequency filters effectively emphasized edge contrasts and enhanced the visibility of subtle linear features.

The structural anomalies identified through topographic analysis were further validated and refined using satellite imagery processed with directional and symmetric matrix filters, as well as a high-frequency Sobel edge-detection filter. This multi-source, integrated approach effectively clarified the linear spectra in the imagery and confirmed the presence of fault structures within the depression (Fig. 2C).

The morphological form of the UKL depression is marked by irregular, non-geometric shapes. Specifically, the northern sector of the depression

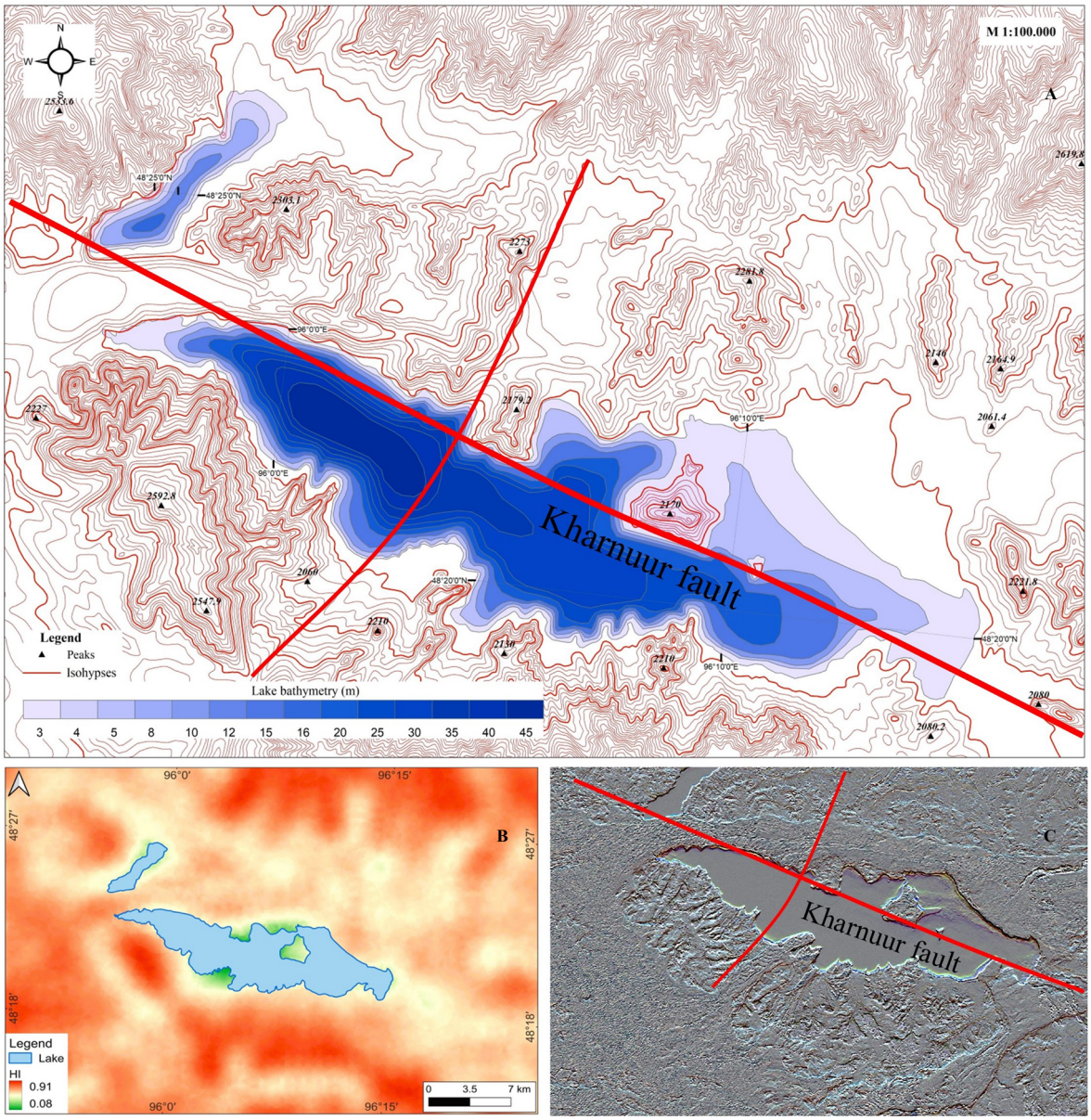

Fig. 2. Topographical and Satellite Image analysis of the study area and fault association. A -Identification of faults through detailed topographic analysis, B -HI analysis of the UKL depression, C -Faults mapped in the UKL area using Sobel filter

exhibits subsidence along a fault zone, while the southern portion shows an uplifted profile, as evidenced by shoreline dissection. These topographical observations suggest significant tectonic influences on the depression's formation. Upon tracing the fault strike, an orthogonal fault was detected, traversing the depression from west to east and from south to north, passing through the lake's central region. The morphological characteristics of the depression further reveal straight-line features, abrupt topographic changes along the fault zones, and stepped contour lines in the lake's bathymetric profile, all indicative of faulting and tectonic activity.

Satellite imagery, processed to enhance linear spectral features, revealed prominent linear patterns that align with the fractures identified in the topographic and geomagnetic data. These spectral anomalies were mapped and cross-validated with geological maps, reinforcing their association with tectonic structures. This approach highlights the utility of satellite imagery in detecting and mapping fault lines, especially in remote and inaccessible regions. The integration of satellite imagery with other geophysical and topographic datasets provides a more comprehensive understanding of the tectonic processes influencing the morphology of the UKL depression.

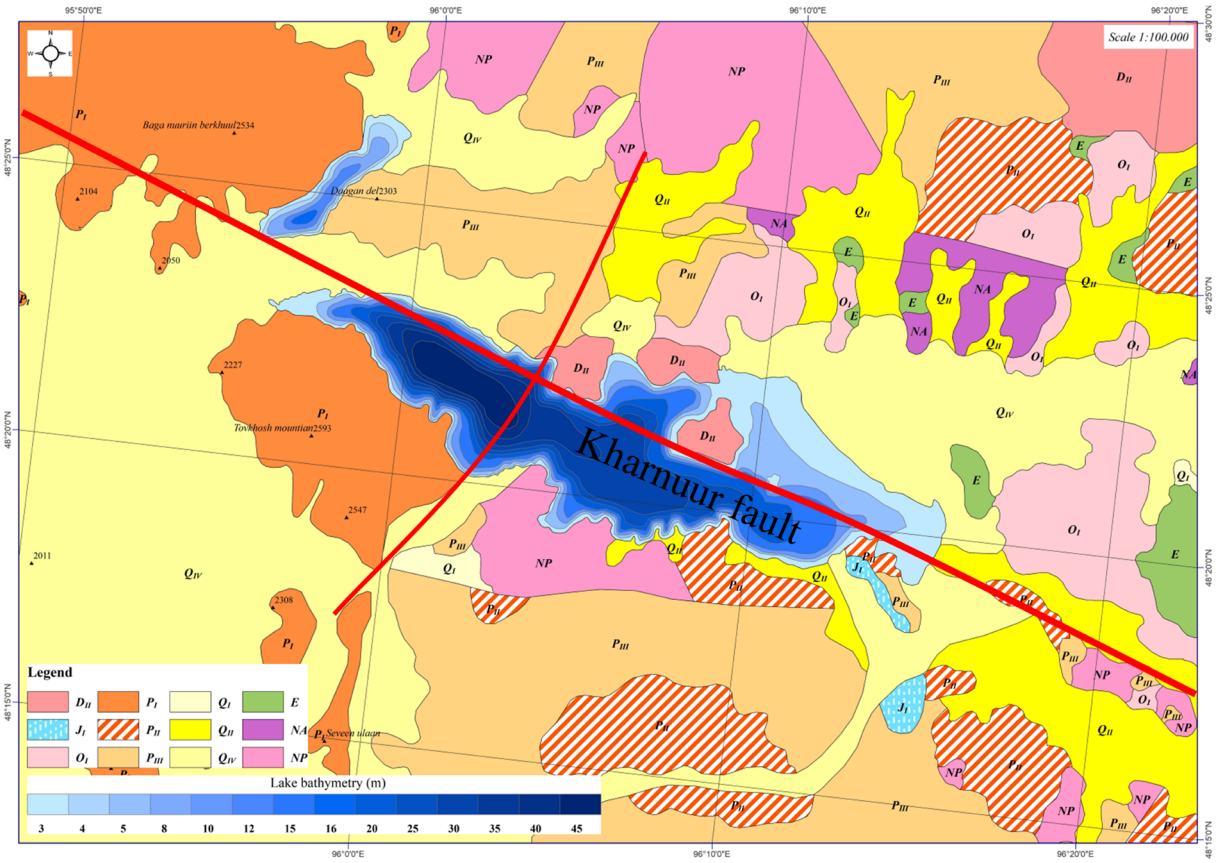

Fig. 3. Geological Faults and Bathymetric Correlation around UKL (Modified after Tumur et al., 2016)

Geological and Bathymetric Map Interpretation: Further insights into the tectonic origins of the UKL depression were gained by overlaying bathymetric data with geological maps. This integration allowed for the identification of subsurface geological features, such as faults, and their intersection with the lake depression. Notable bathymetric anomalies, including sudden depth changes and sharp descents, suggest the presence of faulting or subsidence within the depression. These observations provide evidence of ongoing tectonic processes, such as vertical displacement, which may be altering the lake's depth over time. The geological mapping data, overlaid with the lake's boundaries, bathymetric features, and identified fault lines, corroborate the hypothesis that the depression's morphology is largely shaped by tectonic forces (Fig. 3).

This study employed a combination of morphostructural analysis and spectral enhancement techniques applied to remote sensing data, revealing the presence of a fault crossing the UKL depression, extending over a length of 40.8 km. When bathymetric data of the lake was overlaid on geological maps of the UKL region, it was observed that the fault running through the center of the lake intersected another fault extending toward the western side. The intersection of these faults resulted in a pronounced subsidence of the depression, which in turn caused a significant increase in the lake's depth.

The integration of morphostructural mapping techniques and spectral improvement methods allows for a comprehensive understanding of both surface and subsurface features within the study area. This combined approach provides valuable insights into the relationship between faults and bathymetric anomalies, such as subsidence or fault-induced deepening, offering a clearer picture of both past and present tectonic activities and their impact on the landscape.

Geophysical Interpretation: In addition to the morphostructural analysis, geophysical techniques, including magnetic anomaly mapping and spectral analysis, were employed to further investigate the fault systems within the region. The magnetic anomaly

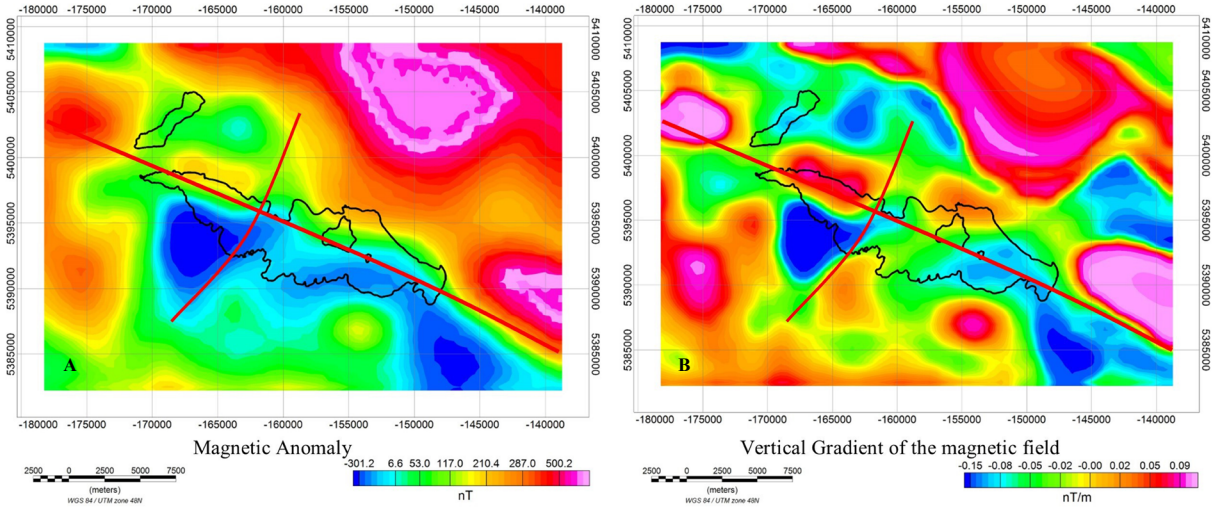

Fig. 4. A -Magnetic anomaly and fault correlation in the study area, B -Vertical Gradient of the magnetic field and fault correlation

data, specifically the magnetic field gradient, was used to identify subsurface geological structures and correlate them with the observed faults. Integrating remote sensing data, such as satellite imagery and bathymetric maps, with geophysical magnetic anomaly data, provides a more nuanced understanding of the fault system and its relationship to the UKL depression. The study also referenced the work of Daariimaa and Baatarchuluun (2017), who used geospherical anomaly data for fault system analysis in Mongolia. A Fourier transform was applied to the magnetic anomaly data from the World Digital Magnetic Anomaly Map, enabling the calculation of local geospherical anomalies specific to the lakes. The relationship between the fault system at UKL and the geophysical magnetic anomalies was further analyzed and presented (Fig. 4).

The vertical gradient of the geomagnetic field serves as a crucial parameter for identifying and characterizing subsurface geological structures, including faults, fractures, and lithological boundaries. In the case of the UKL depression, vertical gradient analysis was applied to enhance the understanding of fault-related anomalies.

The vertical gradient amplifies short-wavelength signals, making it particularly effective for detecting near-surface features. This approach revealed distinct anomalies along the primary fault lines within the lake depression, corresponding to abrupt changes in magnetic field intensity. These anomalies are indicative of underlying structural faults, providing insight into the subsurface geological conditions.

In the study area, the vertical gradient data highlighted two intersecting orthogonal fault systems: one trending northwest to southeast and the other extending north to south. These fault systems exert significant control on the depression's morphology, creating distinct zones of subsidence and uplift, as corroborated by bathymetric and topographic profiles.

Additionally, the vertical gradient anomalies displayed a strong correlation with the lake's bathymetric features, including steep depth variations and linear isobath patterns. This observation further supports the hypothesis that tectonic faulting is the primary driver of the lake's current morphology.

When integrated with geomagnetic and remote sensing data, the vertical gradient analysis provides robust evidence supporting the tectonic origin of the UKL depression. This methodology proves essential for detailed geological and tectonic studies, especially in regions with similar environmental conditions.

Geomagnetic anomalies are invaluable for identifying geological structures such as faults and fractures beneath the surface. For the UKL depression, geomagnetic data were analyzed to establish the relationship between geomagnetic anomalies and faulting within the depression.

The geomagnetic anomaly maps reveal clear

patterns that align with the observed fractures in the lake depression. Vertical gradients of the geomagnetic field were computed to delineate fault parameters, such as depth, orientation, and extent. Fourier transformations of the geomagnetic data further highlighted anomalies corresponding to tectonic features within the study area.

The analysis demonstrated that the primary fractures, trending northwest to southeast and north to south, are strongly associated with significant geomagnetic anomalies. These anomalies suggest variations in lithological composition and structural deformation, likely caused by tectonic forces. The orthogonal configuration of the faulting, as confirmed by the geomagnetic data, aligns with topographic and bathymetric findings, reinforcing the hypothesis that tectonic activity is responsible for the lake depression's formation.

This study underscores the importance of geomagnetic anomaly data in validating and enhancing the understanding of faulting's role in shaping the morphology of lake depressions. The integration of geomagnetic mapping with other geological and remote sensing methods offers a comprehensive approach to studying tectonic influences in such regions.

Relationship Between Faults and Lake Depression Morphology: The morphology of a lake depression is closely tied to tectonic activity, particularly faulting, which can significantly influence both the surface and subsurface features of the depression. Faults, as fundamental structural elements, play a crucial role in shaping the landscape of lake depressions, affecting their depth, shape, and overall topography. The presence of fault systems often leads to the subsidence or uplift of specific areas within the depression, resulting in variations in lake depth and shoreline configuration.

Understanding the relationship between the morphology of lake depressions and the fault systems that influence them is essential

Fig. 5. Field mapping representation of the faults identified in the study area, Photos taken by Altanbold Enkhbold, Tuvshin Gerelmaa

for interpreting the geological evolution of the region, particularly in areas subjected to ongoing tectonic forces.

The main faults identified in the study are depicted in the following photograph (Fig. 5), which illustrates the relationship between fault lines and the overall shape and depth variations within the lake depression. These faults not only define the boundaries of the depression but also contribute to the observed morphological features such as steep isobaths and irregular shoreline dissection.

A detailed geological structural study is necessary to determine the type of fault. In this study, a model was developed to clarify how the faults formed in the lake depressions have affected the morphology of the lake depression (Fig. 6).

A major fault system has formed in the central part of the UKL depression, significantly influencing the lake's morphology. The tectonic movements along this fault have caused the depression to subside from the front to the rear, resulting in the uplift of the northern part of the lake. This uplift has given rise to prominent features such as the Ikh and Baga Abgash Islands, with fault lines observed in front of these islands. The major northwest-southeast (NW-SE) trending fault, which extends 40.8 km in length, exhibits a steep 35° profile, indicating the strong structural control this fault exerts over the depression's formation and current landscape.

The structural configuration along this fault line suggests a connection between tectonic activity and potential groundwater recharge from Late Quaternary and Holocene aquifers. This relationship points to the possibility that tectonic movements have not only shaped the surface morphology of the lake depression but may also influence subsurface hydrological processes, potentially affecting the lake's water supply.

Hydrological Regime and Tectonic Controls on Ulaagchinii Khar Lake: The current state of lakes in Central Asia, including UKL, represents a significant departure from their historical conditions, with notable changes in size and other characteristics over time (Tsegmid, 1969; Walther, 2010; Lehmkuhl et al., 2018). Many of Mongolia's major lakes are remnants of ancient seas or oceans, but the present-day morphology of their depressions varies, and their origins and geological ages differ. Tectonically driven mountain ranges, intermountain depressions, valleys, and lakes formed through faulting are common features in Mongolia, with many of these lakes originating in the early stages of geological history. However, it was during the Quaternary period, marked by significant mountain-building movements, that the modern morphological features of these lake depressions were shaped (Tsegmid, 1969; Doljin and Yembuu, 2021).

Contemporary lakes in Mongolia, such as UKL, continue to be directly influenced by recent tectonic movements, compounded by the impacts of global climate change. Over the past few decades, lake areas across Central Asia have been shrinking, and salinity has increased due to aridification and warming trends. UKL, situated in a semi-arid climate zone, is particularly susceptible to these changes.

Regarding the hydrological regime, UKL receives its surface water primarily from precipitation and both permanent and temporary stream inflows. However, these sources are insufficient to maintain the lake's current volume. Our analysis confirms that the water in UKL remains freshwater, as indicated in (Table 2). This suggests that while hydrological inputs are vital, tectonic factors also play a significant role in the lake's long-term water balance and ecological stability.

Water samples from two locations on UKL the western part (Sample 1) and the eastern part (Sample 2) were compared, and the chemical compositions of both samples were found to be very similar and uniform, indicating consistent water quality across the lake.

The freshwater nature of the lake is primarily due to groundwater that intersects fault lines within the subsided area of the depression. These fault zones facilitate the flow of groundwater into the lake, contributing to the lake's water supply. Carbon-14 (14C) dating of plant pollen samples taken from UKL sediment suggests that the lake is relatively young, approximately 2.7 to 3.5 thousand years old (Sevastyanov et

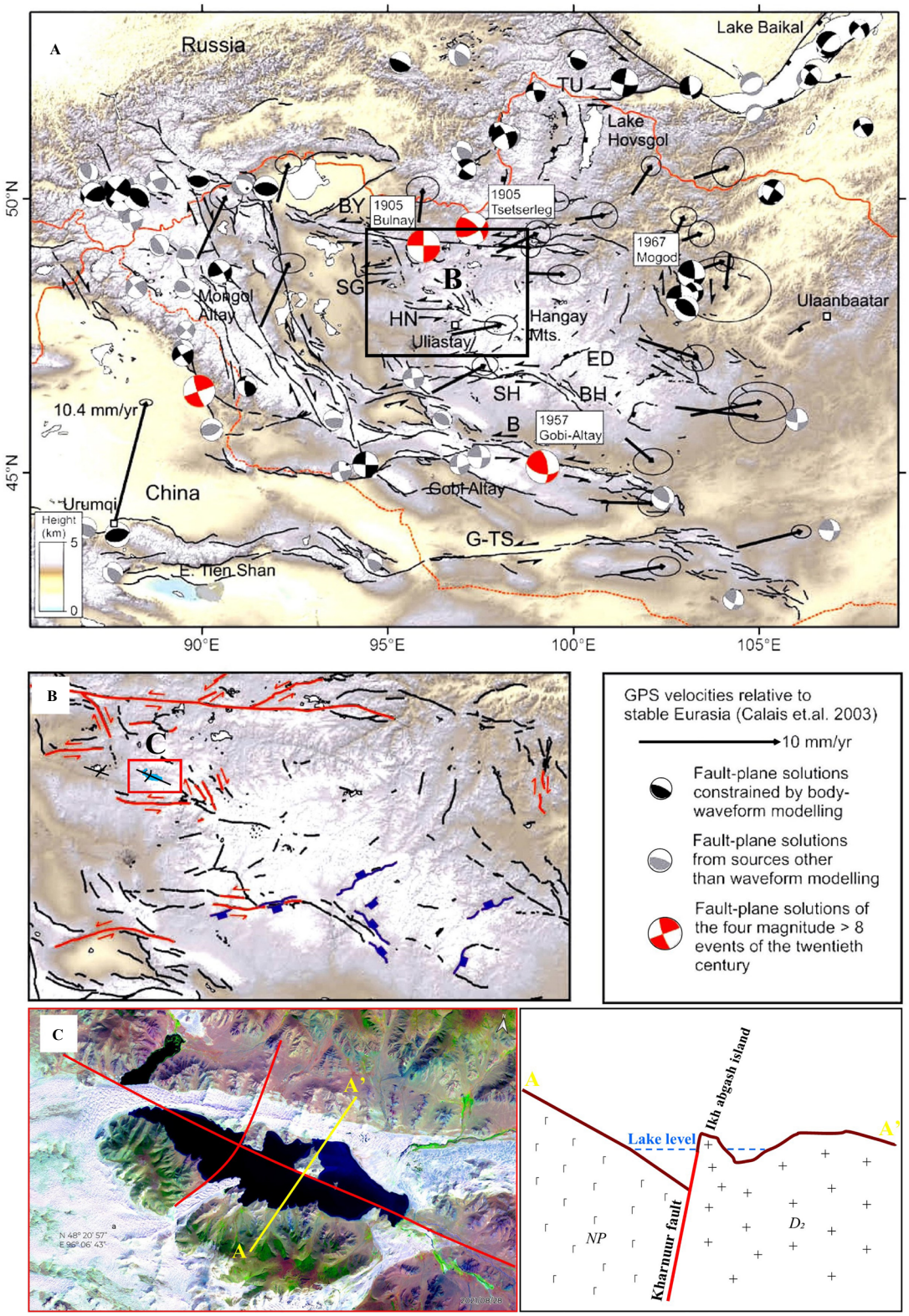

Fig. 6. A -Shaded-relief topographic map of western and central Mongolia derived from SRTM-90 digital elevation data. Active faults are shown as black lines. Major east-west striking strike-slip faults in central Mongolia are labeled as follows: TU -Tunka; BU -Bulnai; SG -Songino-Margats; HN -Khagiin Nuur; SH -South Khangai; B -Bogd; G-TS -Gobi-Tien Shan; ED -Egiin Dawaa; and BH -Bayan Hongor. The names and years of significant historical earthquakes referenced in the text are also indicated (adapted from Bayasgalan et al., 2005; Nissen et al., 2007). B -Enlarged view of the central portion of Fig. 6A, showing the distribution of normal faults (blue) and strike-slip faults (red) that can be confidently identified based on either seismic activity or clear evidence of late Quaternary movement (Modified after Walker et al., 2008). C -Satellite image showing the fault lines near UKL and associated fault patterns related to the uplift of the Khangai Mountains. The A-A' cross-section illustrates the lake depression along the Kharnuur fault. D -Simplified conceptual model illustrating the lake depression and the structural relationship between the associated faults.

Table 2. Chemical analysis results of UKL water

№	Sample parameters and units of measurement	Sampling method designation	MNS 0900:2018	Sample-1	Sample-2
1	pH	MNS ISO 10523:2001	6.5-8.5	8.6	8.5
2	General Khardness, mg-eq/l	MNS ISO 6059:2005	7.0	4.9	4.9
3	Calcium, mg/l	MNS 1097:1970	100.0	56.1	56.1
4	Magnesium, mg/l	MNS 1097:1970	30.0	25.5	25.5
5	Chloride, mg/l	MNS 4424:2005	350	56.8	56.8
6	Hydrocarbonate, mg/l	MNS 6831:2020	-	82.4	61.0
7	Nitrite, mg/l	MNS 4431: 2005	1.0	0.00	0.00
8	Nitrate, mg/l	MNS ISO 7890-3:2001	50.0	14.9	11.6
9	Iron, mg/l	MNS 4430: 2005	0.3	0.00	0.00
10	Ammonium, mg/l	MNS 4428:1997	1.5	0.00	0.00

al., 1994; Tserensodnom, 2000). However, there is a need for further studies using modern dating techniques on the lake's sedimentary layers to refine our understanding of the lake's exact age. While the age of the sediments remains uncertain, neotectonic movements have significantly influenced the current morphology of the depression, shaping the lake's surface features. These movements, driven by fault activity, have caused both uplifting and subsiding of the depression, further contributing to its present-day topography (Selivanov, 1972; Sevastyanov et al., 1994; Tserensodnom, 2000). Additionally, sediment accumulation and sand displacement have also played a role in shaping the lake's geomorphological structure.

Hydrogeological studies provide insight into the groundwater conditions surrounding UKL. Groundwater is present at varying depths along the edges of the Bor Khayr dune, with groundwater levels ranging from 5 to 10 m. In the center of the sand dunes, groundwater can be found at depths up to 50 m, with deeper groundwater occurring below this level (Jadambaa, 2009). Notably, the depth of the groundwater corresponds to the depth of the lake itself, suggesting a connection between groundwater and the lake's water supply.

Based on these observations, it is hypothesized that the groundwater feeding UKL likely originates from Late Quaternary and Holocene-aged aquifers along fault lines. However, further research is needed to identify the specific sources of the lake's water and to determine the contribution of each source to the lake's overall water balance. Understanding these interactions will provide valuable insights into the hydrogeological dynamics of the region and the factors influencing the lake's hydrology.

The Shape of Ulaagchinii Khar Lake and the Influence of Sand Dynamics: The morphological characteristics of UKL and the surrounding spatial distribution of sand dunes reveal a dynamic interaction between tectonic forces and aeolian processes, which have significantly shaped the current landscape. The Bor Khyar dune system, which extends southeastward from the Khyargas Lake depression, exemplifies the impact of westerly sediment transport in this region. This dune system is expansive, with a width ranging from 30 to 40 km, a length of approximately 250 km, and a thickness between 120 and 170 m, reflecting sustained and large-scale aeolian activity during the Late Quaternary (Klein, 2001; Grunert and Lehmkuhl, 2004; Enkhbold et al., 2022b).

The presence of sand dunes along the northern, southwestern, and southeastern margins of UKL highlights the complex interplay between sediment accumulation and the lake's hydrodynamics. These dunes, which have been dated to the Pleistocene and Holocene periods, indicate that aeolian processes have been active throughout the Late Quaternary (Grunert et al., 2000; Walther, 2010; Klinge and Sauer, 2019; Klinge et al., 2022). The movement and deposition of sand have been pivotal in modifying the morphology of the lake depression.

While the primary structural control of the UKL depression is attributed to tectonic faulting, evidenced by recent uplift and subsidence, the contribution of sand dynamics to the lake's evolving morphology cannot be ignored. The narrowing of the depression and the apparent separation between Baga Lake and UKL may have been influenced by dune accumulation in the Us Zuudug Els corridor. Additionally, the deposition of sands from the Elst Shanaa dune field into the southwestern part of the depression seems to have altered the shoreline configuration of the lake and possibly affected the hydrological connectivity of UKL (Fig. 7).

This interplay between tectonic and aeolian processes demonstrates the multifaceted evolution of the UKL depression. While tectonic activity has shaped the primary structure of the lake, the aeolian dynamics of sand transport and deposition have played an essential role in further modifying the landscape, affecting both the lake's morphology and its hydrological characteristics. Further investigation into these processes will be crucial for understanding the long-term evolution of the lake depression and its surrounding environment.

These findings underscore the importance of considering both tectonic and aeolian drivers in assessing the geomorphological evolution of closed-basin lakes in arid and semi-arid regions of Central Asia.

These findings highlight the critical need to consider both tectonic and aeolian processes

Fig. 7. Sand dunes that have influenced the shape of UKL. A -Us Zuudug Els dunes distributed along the northern shoreline. B, C and D -Aeolian Els Shanaa dunes transported from the southwestern side of the lake (Photo by Erdenebulgan Battsengel, Altanbold Enkhbold)

when evaluating the geomorphological evolution of closed-basin lakes, particularly in arid and semi-arid regions of Central Asia. Understanding how these two drivers interact can provide deeper insights into the formation and transformation of these landscapes. As seen with UKL, the combined effects of faulting, uplift, subsidence, and aeolian sand dynamics have played an integral role in shaping the lake's morphology and hydrology.

Future work integrating high-resolution topographic data and stratigraphic analysis could help further delineate the relative contributions of these processes to the observed landforms.

CONCLUSION

The origin and morphological features of the Ulaagchinii Khar Lake depression are confirmed to be independent of aeolian processes and are instead associated with the development of orthogonal fault systems within the depression. In this study, fault zones within the lake depression were identified through morphometric analysis, advanced remote sensing techniques, and integrated geophysical magnetic mapping.

The morphometric analysis of the UKL depression reveals *HI*=0.91, *Bs*=2.81, *RSl*=35°, and *Re*=274 m. These indicators collectively suggest significant tectonic control in the formation of the depression.

The results indicate that orthogonal faults, oriented from the southwest to the northeast and from the south to the west across the central part of the lake depression, have shaped the current morphology. Tectonic movements along these faults have influenced the formation of the lake depression's present appearance.

Subsidence occurred along meridionally oriented faults, resulting in the formation of the lake depression, while uplift in the northern part of the surface led to the emergence of the Ikh and Baga Abgash Islands.

The morphological model of the lake depression, when examined alongside faulting patterns, provides valuable insights into the tectonic history of the region. Faults often have a significant impact on the development and characteristics of the lake depression, influencing its shape, depth, and surrounding structural features. The present morphology of UKL reflects a combined influence of tectonic deformation and aeolian sand accumulation, which together have significantly shaped the lake's hydrological structure and depression configuration.

By studying these relationships, we can better understand the dynamic forces shaping the landscape and predict how ongoing tectonic activity might continue to affect the lake's evolution. This provides the potential for a more detailed differentiation of the factors influencing changes in lake water regimes, volumes, and surface areas, which underscores the significance of this research.

ACKNOWLEDGEMENTS

This study was carried out as part of the basic research project "Geomorphological new subdivisions of lake districts in Mongolia" implemented by the Mongolian Foundation for Science and Technology from 2024 to 2026.

Conflicts of interest

The authors declare that they have no conflicts of interest.

Data availability statement

This study used Satellite data that were publicly available from the United States Geological Survey (USGS) (https://www.usgs.gov/). The data that support the findings of this study are available from the first and corresponding author, upon reasonable request.

REFERENCE

Anand, A.K., Pradhan, S.P. 2019. Assessment of active tectonics from geomorphic indices and morphometric parameters in part of Ganga basin. Journal of Mountain Science, vol. 16(8), p. 1943-1961. https://doi.org/10.1007/s11629-018-5172-2

Bayasgalan, A., Jackson, J., McKenzie, D. 2005. Lithosphere rheology and active tectonics in Mongolia: relations between earthquake source parameters, gravity and GPS measurements. Geophysical Journal International, vol. 163(3), p. 1151-1179. https://doi.org/10.1111/j.1365-246X.2005.02764.x

Bayasgalan, A., Jackson, J., Ritz, J.F., Carretier, S. 1999. Forebergs', flower structures, and the development of large intra-continental strike-slip faults: the Gurvan Bogd fault system in Mongolia. Journal of Structural Geology, vol. 21(10), p. 1285-1302. https://doi.org/10.1016/S0191-8141(99)00064-4

Boyce, J.I., Pozza, M.R., Morris, W.A., Eyles, N., Doughty, M. 2002. High-Resolution Magnetic and Seismic Imaging of Basement Faults in Western Lake Ontario and Lake Simcoe, Canada. Symposium on the Application of Geophysics to Engineering and Environmental Problems, 2002, p. 191-194 https://doi.org/10.4133/1.2927124

Byamba, J. 2009. Lithospheric Plate Tectonics. Byamba, J (Ed.) Geology and Mineral Resources of Mongolia, vol. IV, Soyombo Printing, Ulaanbaatar, p. 126-128. (in Mongolian)

Canty, M.J. 2014. Image Analysis, Classification and Change Detection in Remote Sensing. With Algorithms for ENVI/IDL and Python, Third Edition. CRC Press, p. 244-349 https://doi.org/10.1201/b17074

Carretier, S., Ritz, J.F., Jackson, J. Bayasgalan, A. 2002. Morphological dating of cumulative reverse fault scarps: examples from the Gurvan Bogd fault system, Mongolia. Geophysical Journal International, vol. 148(2), p. 256-277. https://doi.org/10.1046/j.1365-246X.2002.01007.x

Cohen, A.S. 2003. Paleolimnology: The History and Evolution of Lake Systems. Oxford University Press. https://doi.org/10.1093/oso/9780195133530.001.0001

Cunningham, D. 2005. Active intracontinental transpressional mountain building in the Mongolian Altai: defining a new class of orogen. Earth and Planetary Science Letters, vol. 240(2), p. 436-444. https://doi.org/10.1016/j.epsl.2005.09.013

Cunningham, D. 2013. Mountain building processes in intracontinental oblique deformation belts: Lessons from the Gobi Corridor, Central Asia. Journal of Structural Geology, vol. 46, p. 255-282. https://doi.org/10.1016/j.jsg.2012.08.010

Cunningham, D., Davies, S., Badarch, G. 2003. Crustal architecture and active growth of the Sutai Range, western Mongolia: a major intracontinental, intraplate restraining bend. Journal of Geodynamics, vol. 36(1-2), p. 169-191. https://doi.org/10.1016/S0264-3707(03)00046-2

Daarimaa, B., Baatarchuluun, Ts. 2017. Evaluation of the tectonic fault system of Mongolia based on geomagnetic anomaly fields. Geological Issues, vol. 15(01), p. 58–67. (In Mongolian with English abstract) https://journal.num.edu.mn/geology/article/view/2273

Das, B.C., Islam, A., Sarkar, B. 2022. Drainage Basin Shape Indices to Understanding Channel Hydraulics. Water Resources Management, vol. 36(8), p. 2523-2547. https://doi.org/10.1007/s11269-022-03121-4

Di Crescenzo, G., Santo, A. 2005. Debris slides-rapid earth flows in the carbonate massifs of the Campania region (Southern Italy): morphological and morphometric data for evaluating triggering susceptibility. Geomorphology, vol. 66(1-4), p. 255-276. https://doi.org/10.1016/j.geomorph.2004.09.015

Doljin, D., Yembuu, B. 2021. The relief and geomorphological characteristics of Mongolia. In: Yembuu, B. (eds) The Physical Geography of Mongolia, Springer International Publishing, p. 23-50. https://doi.org/10.1007/978-3-030-61434-8_3

El Hamdouni, R., Irigaray, C., Fernandez, T., Chacón, J., Keller, E.A. 2008. Assessment of relative active tectonics, southwest border of the Sierra Nevada (southern Spain). Geomorphology, vol. 96(1-2), p. 150-173. https://doi.org/10.1016/j.geomorph.2007.08.004

Enkhbold, A., Dorjsuren, B., Khukhuudei, U., Yadamsuren, G., Bardarch, D., Dorjgochoo, S., Gonchigjav, Y., Nyansuren, D., Ragchaa, G., Gedefaw, M. 2021b. Impact of faults on the origin of lake depressions: a case study of Bayan Nuur depression, North-west Mongolia, Central Asia. Geografia Fisica e Dinamica Quaternaria, vol. 44(1), p. 53-66. https://www.gfdq.glaciologia.it/index.php/gfdq/article/view/30

Enkhbold, A., Khukhuudei, U., Doljin, D. 2021a. Morphological classification and origin of lake depressions in Mongolia. Proceedings of the Mongolian Academy of

Sciences, vol. 61(02), p. 35-43. https://doi.org/10.5564/pmas.v61i02.1758

Enkhbold, A., Khukhuudei, U., Doljin, D. 2024b. New geomorphological districts of lakes in Mongolia. Mongolian Journal of Geography and Geoecology, vol. 61(45), p. 1-18. (In Mongolian with English abstract) https://doi.org/10.5564/mjgg.v61i45.3235

Enkhbold, A., Khukhuudei, U., Kusky, T., Chun, X., Yadamsuren, G., Ganbold, B., Gerelmaa, T. 2022c. Morphodynamic development of the Terkhiin Tsagaan lake depression, Central Mongolia: implications for the relationships of faulting, volcanic activity, and lake depression formation. Journal of Mountain Science, vol. 19(9), p. 2451-2468. https://doi.org/10.1007/s11629-021-7144-1

Enkhbold, A., Khukhuudei, U., Kusky, T., Tsermaa, B., Doljin, D. 2022b. Depression morphology of Bayan Lake, Zavkhan province, Western Mongolia: implications for the origin of lake depression in Mongolia. Physical Geography, vol. 43(6), p. 1-26. https://doi.org/10.1080/02723646.2021.1899477

Enkhbold, A., Khukhuudei, U., Seong, Y.B., Gonchigjav, Y., Dingjun, L., Ganbold, B. 2024a. Geomorphological study of the origin of Mongolian Altai Mountains Lake depressions: implications for the relationships between tectonic and glacial processes. Mongolian Geoscientist, vol. 29(58), p. 1-18. https://doi.org/10.5564/mgs.v29i58.3237

Farhan, Y., Mousa, R., Dagarah, A., Shtaya, D. 2016. Regional Hypsometric Analysis of the Jordan Rift Drainage Basins (Jordan) Using Geographic Information System. Open Journal of Geology, vol. 6(10), p. 1312-1343. https://doi.org/10.4236/ojg.2016.610096

Filosofov, V.P. 1967. The value of the map of potential relief energy for geomorphological and Neotectonic studies. Methods geomorphological. Novosibirsk: Science. Siberian Department. p. 193-198 (in Russian)

Florinsky, I.V. 1996. Quantitative topographic method of fault morphology recognition. Geomorphology, vol. 16(2), p. 103-119. https://doi.org/10.1016/0169-555X(95)00136-S

Ganas, A., Pavlides, S., Karastathis, V. 2005. DEM-based morphometry of range-front escarpments in Attica, central Greece, and its relation to fault slip rates. Geomorphology, vol. 65(3-4), p. 301-319. https://doi.org/10.1016/j.geomorph.2004.09.006

Gilvear, D., Bryant, R. 2016. Analysis of remotely sensed data for fluvial geomorphology and river science. Kondolf, G.M. and Piégay, H (Eds.). Tools in fluvial geomorphology, Chapter 6, p. 103-132. https://doi.org/10.1002/9781118648551.ch6

Grunert, J., Lehmkuhl, F. 2004. Aeolian sedimentation in arid and semi-arid environments of Western Mongolia. In: Smykatz-Kloss, W., Felix-Henningsen, P. (Eds) Paleoecology of Quaternary drylands. Berlin, Heidelberg: Springer Berlin Heidelberg, p. 195-218. https://doi.org/10.1007/978-3-540-44930-0_11

Grunert, J., Lehmkuhl, F., Walther, M. 2000. Paleoclimatic evolution of the Uvs Nuur basin and adjacent areas (Western Mongolia). Quaternary International, vol. 65-66, p. 171-192. https://doi.org/10.1016/S1040-6182(99)00043-9

Hassen, M.B., Deffontaines, B., Turki, M.M. 2014. Recent tectonic activity of the Gafsa fault through morphometric analysis: Southern Atlas of Tunisia. Quaternary International, vol. 338, p. 99-112. https://doi.org/10.1016/j.quaint.2014.05.009

Hooper, D.M., Bursik, M.I., Webb, F.H. 2003. Application of high-resolution, interferometric DEMs to geomorphic studies of fault scarps, Fish Lake Valley, Nevada-California, USA. Remote Sensing of Environment, vol. 84(2), p. 255-267. https://doi.org/10.1016/S0034-4257(02)00110-4

Jacques, P.D., Salvador, E.D., Machado, R., Grohmann, C.H., Nummer, A.R. 2014. Application of morphometry in neotectonic studies at the eastern edge of the Paraná Basin, Santa Catarina State, Brazil. Geomorphology, vol. 213, p. 13-23. https://doi.org/10.1016/j.geomorph.2013.12.037

Jadambaa, N. 2009. Hydrogeology. Byamba, J. (Ed.) Geology and Mineral Resources of Mongolia, vol. VIII, Soyombo Printing, Ulaanbaatar, p. 215-216. (in Mongolian)

Jensen, J.R. 1996. Introductory Digital Image

Processing: A Remote Sensing Perspective, Second Edition, Prentice-Hall Inc., p. 233-239. ISBN0-13-145361-0

Karatas, A., Boulton, S. 2019. Morphometric characteristics of alluvial fans in Southern Turkey: implications for fault activity in the Anatolia, Arabia, Africa Triple Junction Region. Academia Journal of Environmental Sciences, vol. 7(3), p. 9-29. https://pearl.plymouth.ac.uk/gees-research/704/

Klein, M. 2001. Inland dunes in northern Central Asia. Uvs Nuur Basin, northwestern Mongolia. Geographical Institute of the Johannes Gutenberg University, p.116-124 (in German)

Klinge, M., Sauer, D. 2019. Spatial pattern of Late Glacial and Holocene climatic and environmental development in Western Mongolia-a critical review and synthesis. Quaternary Science Reviews, vol. 210, p. 26-50. https://doi.org/10.1016/j.quascirev.2019.02.020

Klinge, M., Schneider, F., Li, Y., Frechen, M., Sauer, D. 2022. Variations in geomorphological dynamics in the northern Khangai Mountains, Mongolia, since the Late Glacial period. Geomorphology, vol. 401, 108113. https://doi.org/10.1016/j.geomorph.2022.108113

Lamb, M.A., Hanson, A.D., Graham, S.A., Badarch, G. Webb, L.E. 1999. Left-lateral sense offset of upper Proterozoic to Paleozoic features across the Gobi Onon, Tost, and Zuunbayan faults in southern Mongolia and implications for other Central Asian faults. Earth and Planetary Science Letters, vol. 173(3), p. 183-194. https://doi.org/10.1016/S0012-821X(99)00227-7

Launay, M., Guerif, M. 2005. Assimilating remote sensing data into a crop model to improve predictive performance for spatial applications. Agriculture, Ecosystems & Environment, vol. 111(1-4), p. 321-339. https://doi.org/10.1016/j.agee.2005.06.005

Lehmkuhl, F., Grunert, J., Hülle, D., Batkhishig, O., Stauch, G. 2018. Paleolakes in the Gobi region of southern Mongolia. Quaternary Science Reviews, vol. 179, p. 1-23. https://doi.org/10.1016/j.quascirev.2017.10.035

Maliqi, E., Kumar, N., Latifi, L., Singh, S.K. 2023. Soil Erosion Estimation Using an Empirical Model, Hypsometric Integral and Geo-Information Science - A Case Study. Ecological Engineering & Environmental Technology, vol, 24(4), p. 62-72. https://doi.org/10.12912/27197050/161957

Mats, V.D. 1993. The structure and development of the Baikal rift depression. Earth-Science Reviews, vol. 34(2), p. 81-118. https://doi.org/10.1016/0012-8252(93)90028-6

Nissen, E., Emmerson, B., Funning, G.J., Mistrukov, A., Parsons, B., Robinson, D.P., Wright, T.J. 2007. Combining InSAR and seismology to study the 2003 Siberian Altai earthquakes—dextral strike-slip and anticlockwise rotations in the northern India–Eurasia collision zone. Geophysical Journal International, vol. 169(1), p. 216-232. https://doi.org/10.1111/j.1365-246X.2006.03286.x

Nixon, M., Aguado, A. 2019. Feature Extraction and Image Processing for Computer Vision. Academic Press is an imprint of Elsevier, p. 344-356. eBook ISBN: 9780128149775

Onorato, M.R., Coronato, A., Perucca, L.P., Rabassa, J., López, R. 2017. Morpho-bathymetry and surficial morphology of Udaeta Lake, along the Magallanes-Fagnano fault system, Tierra del Fuego, Argentina. Journal of South American Earth Sciences, vol. 76, p. 1-10. https://doi.org/10.1016/j.jsames.2017.02.001

Phillips, J.D. 2000. Locating magnetic contacts: A comparison of the horizontal gradient, analytic signal, and local wavenumber methods. SEG Technical Program Expanded Abstracts, p. 402-405. https://doi.org/10.1190/1.1816078

Salem, A., Williams, S., Fairhead, D., Smith, R., Ravat, D. 2008. Interpretation of magnetic data using tilt-angle derivatives. Geophysics, vol. 73(1), p. 14JF-Z11. https://doi.org/10.1190/1.2799992

Samozvantsev, B.A., Tsukernik, A.B., Golyakov, B.I. 1981. Results of 1:200 000 scale geological mapping and general prospecting in Great Lakes depression of western branches of Khangay Highland. Ulaanbaatar, Geologic Information Center Open-File Report #3576, 1036 p.

Selivanov, E.I. 1972. Neotectonics and

Geomorphology of the Mongolian People's Republic, Nedra, p. 231-244 (in Russian)

Sevastyanov, D.V., Shuvalov, V.F., Neustrueva, I.Y. 1994. Limnology and Paleolimnology of Mongolia. St. Petersburg, p. 59-94 (in Russian)

Shamir, G. 2006. The active structure of the Dead Sea Depression. Special Papers-Geological Society of America, vol. 401, p. 15-27. https://doi.org/10.1130/2006.2401(02)

Shinneman, A.L., Almendinger, J.E., Umbanhowar, C.E., Edlund, M.B., Nergui, S. 2009. Paleolimnologic evidence for recent eutrophication in the Valley of the Great Lakes (Mongolia). Ecosystems, vol. 12(6), p. 944-960. https://doi.org/10.1007/s10021-009-9269-x

Strahler, A.N. 1964. Quantitative Geomorphology of Drainage Basin and Channel Networks. In: Chow, V. (Ed.) Handbook of Applied Hydrology, McGraw Hill, New York, p. 439-476.

Studinger, M., Karner, G.D., Bell, R.E., Levin, V., Raymond, C.A., Tikku, A.A. 2003. Geophysical models for the tectonic framework of the Lake Vostok region, East Antarctica. Earth and Planetary Science Letters, vol. 216(4), p. 663-677. https://doi.org/10.1016/S0012-821X(03)00548-X

Theilen-Willige, B., Aher, S.P., Gawali, P.B., Venkata, L.B. 2016. Seismic hazard analysis along Koyna Dam area, western MaKharashtra, India: A contribution of remote sensing and GIS. Geosciences, vol. 6(2), 20. https://doi.org/10.3390/geosciences6020020

Tsagaan, B., Chimed, O., Tsermaa, B., Khukhuudei, U. 2024. The crustal thickness and Vp/Vs ratio in Mongolia. Geodynamics & Tectonophysics, vol. 15(4), 6. https://doi.org/10.5800/GT-2024-15-4-0771

Tsegmid, S. 1969. Physical geography of Mongolia. Mongolian Academy of Sciences, Institute of Geography and Permafrost. Ulaanbaatar, Mongolia. p. 23-103 (in Mongolian)

Tserensodnom, J. 1971. Lakes of Mongolia. Mongolian Academy of Sciences, Institute of Geography and Permafrost. Ulaanbaatar, Mongolia, p. 7-54 (in Mongolian)

Tserensodnom, J. 2000. Catalog of lakes of Mongolia. Mongolian Academy of Sciences, Institute of Geography and Permafrost. Ulaanbaatar, Mongolia p. 55-109 (in Mongolian)

Tumur, S., Batmunkh, E., Ganbat, Ch., Jargal, O., Batsukh, E., Munkhbat. P. 2016. Songino-Tarvagatai- Baidrag (M-47-XXXI) series, geological map scale 1:200 000. Tumurtogoo, O., Dorjnamjaa, D., Orolmaa, D., Chuluun, D., Ariunchimeg. Ya. (Eds.) Mongolian Geodatabase, Magma Mines LLC, Mineral Resources and Petroleum Authority of Mongolia, Ministry of Mining and Heavy Industry.

Walker, R.T., Molor, E., Fox, M., Bayasgalan, A. 2008. Active tectonics of an apparently aseismic region: distributed active strike-slip faulting in the Hangay Mountains of central Mongolia. Geophysical Journal International, vol. 174(3), p. 1121-1137. https://doi.org/10.1111/j.1365-246X.2008.03874.x

Walker, R.T., Nissen, E., Molor, E., Bayasgalan, A. 2007. Reinterpretation of the active faulting in central Mongolia. Geology, vol. 35(8), p. 759-762. https://doi.org/10.1130/G23716A.1

Walther, M. 2010. Paleo-Environmental Changes in the Uvs Nuur Basin (Northwest-Mongolia). Exploration into the Biological Resources of Mongolia, p. 267-279. ISSN 0440-1298

Yang, X., Li, W., Qin, Z. 2015. Calculation of reverse-fault-related parameters using topographic profiles and fault bedding. Geodesy and Geodynamics, vol. 6(2), p. 106-112. https://doi.org/10.1016/j.geog.2014.09.002